RHIC ISOBAR RESULTS AND IMPLICATION ON NUCLEAR STRUCTURE

HAOJIE XU (徐浩洁)

HUZHOU UNIVERSITY(湖州师范学院)

IN COLLABORATION WITH:

LIE-WEN CHEN, HANLIN LI, ZIWEI LIN, SHI PU, CAIWAN SHEN, FUQIANG WANG,

JIANFEI WANG, XIAOBAO WANG, HANZHONG ZHANG, JIE ZHAO, WENBIN ZHAO, YING ZHOU.

RBRC VIRTUAL WORKSHOP: PHYSICS OPPORTUNITIES FROM THE RHIC ISOBAR RUN

JANUARY 25-28, 2022, BNL

Outline

- Importance of isobar structure on the CME search
- Probing the nuclear structure with isobar collisions
  - Neutron skin
  - Initial fluctuation/correlations
  - Nuclear deformation (Giuliano, Chunjian, …)
- Summary

Relativistic Heavy ion collisions

Woods-Saxon distributions

$$\rho(r) = \frac{\rho_0}{1 + \exp[(r - R)/a]}$$

$$R = R_0\,[1+\beta_2 Y_2^0(\theta)+\beta_4 Y_4^0(\theta)]$$

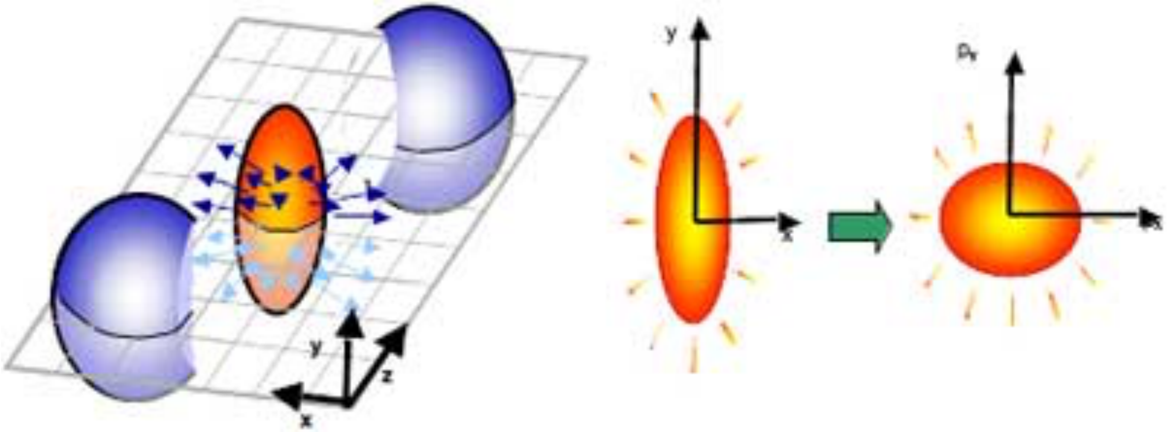

Anisotropic flow,
Flow fluctuations
HBT,
....

Bulk properties of QGP medium: $\eta/s, \zeta/s, \ldots$

Initial geometry

Final observables

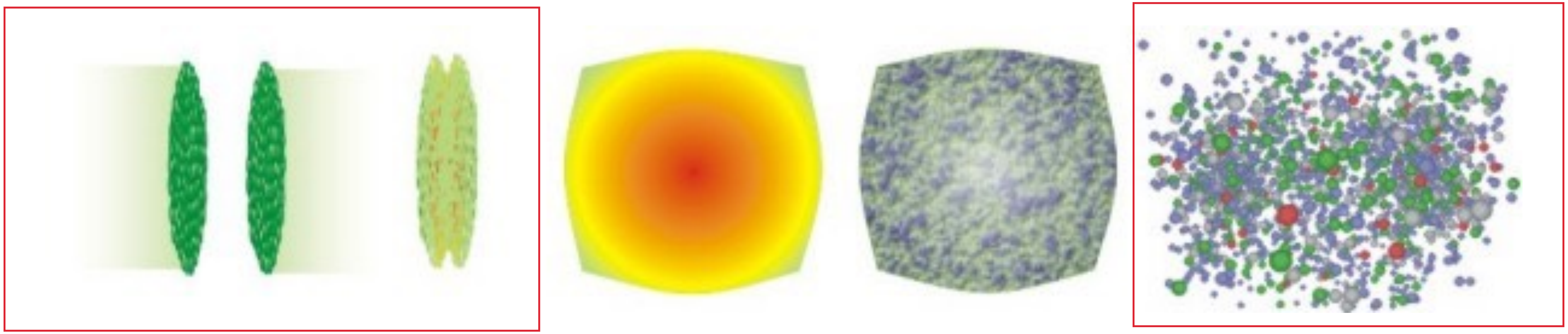

Relativistic isobaric collisions and chiral magnetic effect

Chiral magnetic effect (CME)

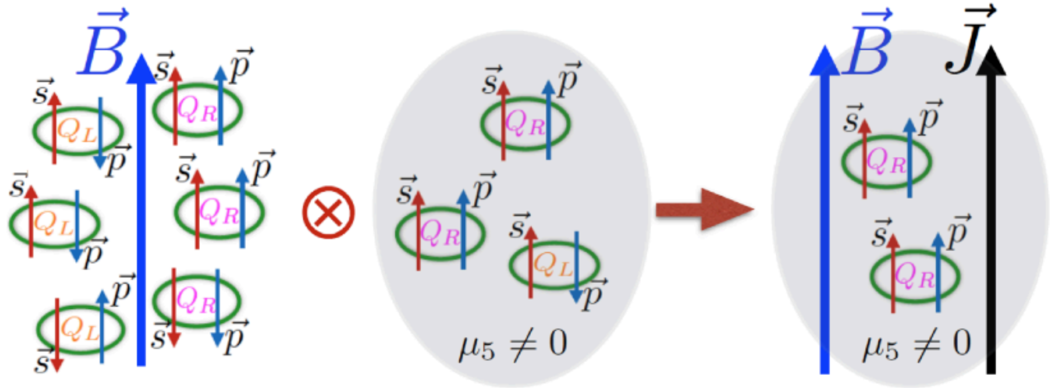

$$\gamma \equiv \langle \cos(\varphi_\alpha + \varphi_\beta - 2\Psi_{RP}) \rangle$$

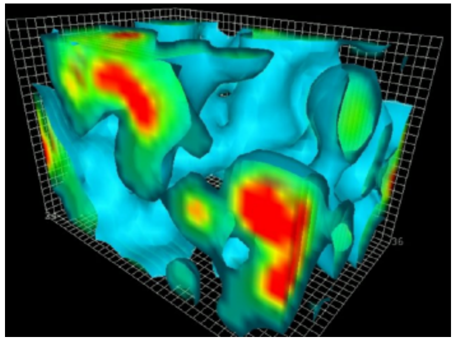

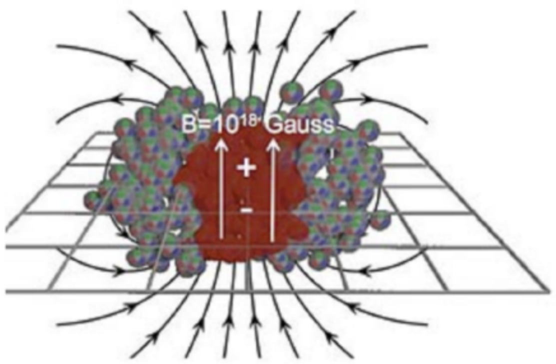

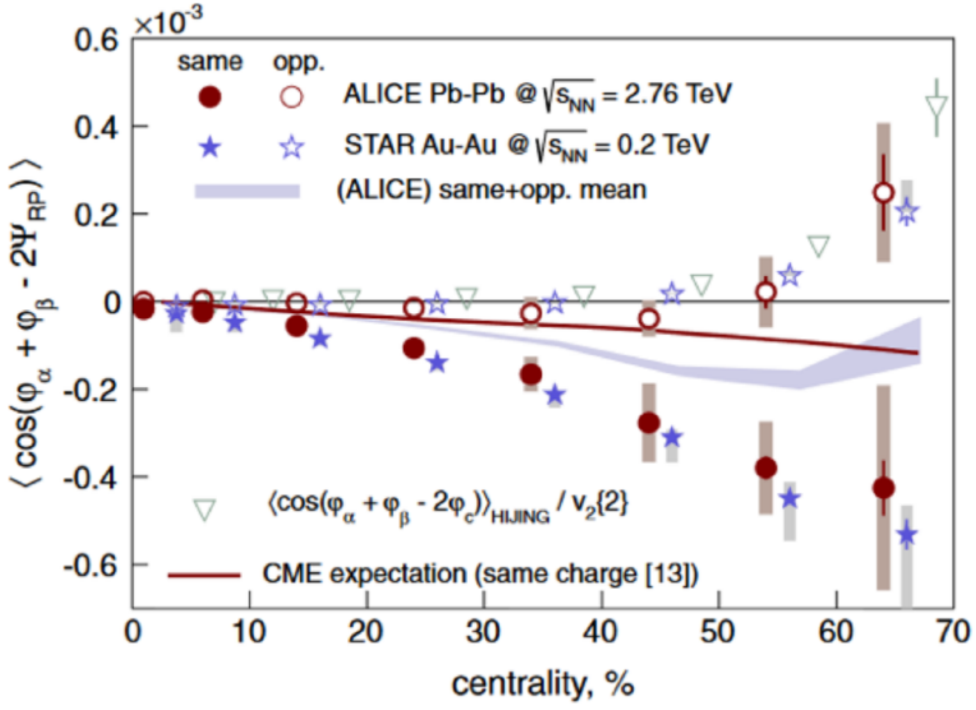

$$\mathbf{J}_{\mathbf{cme}} = \sigma_5 \mathbf{B} = \left(\frac{(Qe)^2}{2\pi^2} \mu_5 \right) \mathbf{B},$$

D. Kharzeev,et.al., PPNP88, 1(2016)

STAR, PRL103, 251601 (2009)
ALICE, PRL110, 012301 (2013)

Relativistic isobaric collisions and chiral magnetic effect

Background issue

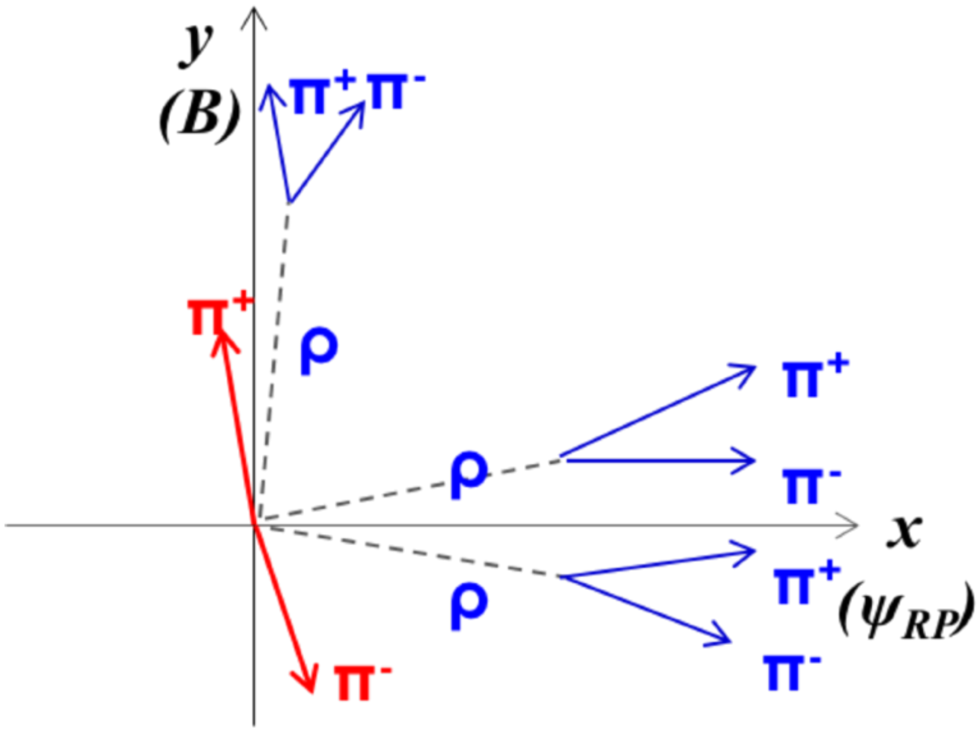

The isobar collisions was proposed to measure the chiral magnetic effect.

S. Voloshin, PRL105, 172301 (2010)

$_{40}^{96}Zr + _{40}^{96}Zr$ $\quad$ $_{44}^{96}Ru + _{44}^{96}Ru$

$$\sqrt{s_{NN}} = 200\text{ GeV}$$

- Same geometry
  - Same eccentricities => same flow background
  - Same multiplicity for a given impact parameter
- Same decay kinematics
- Different magnetic field => different CME signals

$$\Delta\gamma_{\text{bkg}} = \langle\cos(\varphi_\alpha + \varphi_\beta - 2\Psi_{RP})\rangle = \frac{N_{\text{cluster}}}{N_\alpha N_\beta} \times \langle\cos(\varphi_\alpha + \varphi_\beta - 2\Psi_{\text{cluster}})\rangle \times v_{2,\text{cluster}}$$

Relativistic isobaric collisions and chiral magnetic effect

	R	a	beta2
Zr	5.02	0.46	0.08/0.217
Ru	5.085	0.46	0.158/0.053

WS parameters extracted from charge density distributions

W. Deng, X. Huang, et.al., PRC94,041901(2016)

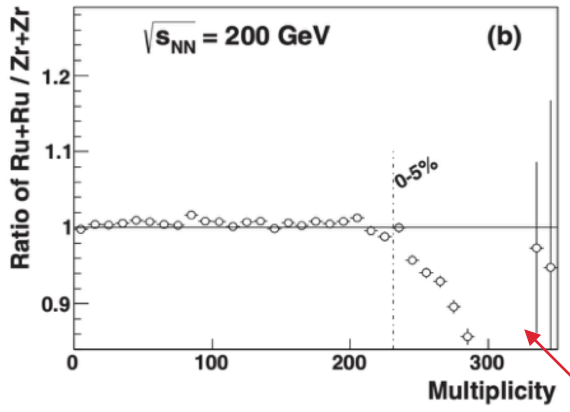

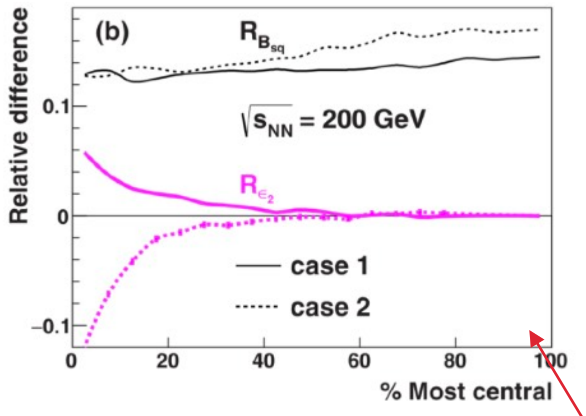

$$\Delta\gamma_{\text{bkg}} = \langle\cos(\varphi_\alpha + \varphi_\beta - 2\Psi_{RP})\rangle = \frac{N_{\text{cluster}}}{N_\alpha N_\beta} \times \langle\cos(\varphi_\alpha + \varphi_\beta - 2\Psi_{\text{cluster}})\rangle \times v_{2,\text{cluster}}$$

2010 The isobar method was proposed. S. Voloshin, PRL105, 172301 (2010)

2016 The method was verified by model study. W. Deng, X. Huang, et.al, PRC94, 041901 (2016)

2017 The importance of isobar structure was investigated. HJX, et.al., PRL121, 022301 (2018)

2018 The isobar data are taken by the STAR collaboration.

2021 The first CME results published by the STAR collaboration, confirm the isobar structure differences. STAR, PRC105, 014901 (2022)

Isobar structures are important for the CME search

STAR, Isobar, PRC105, 014901(2022)

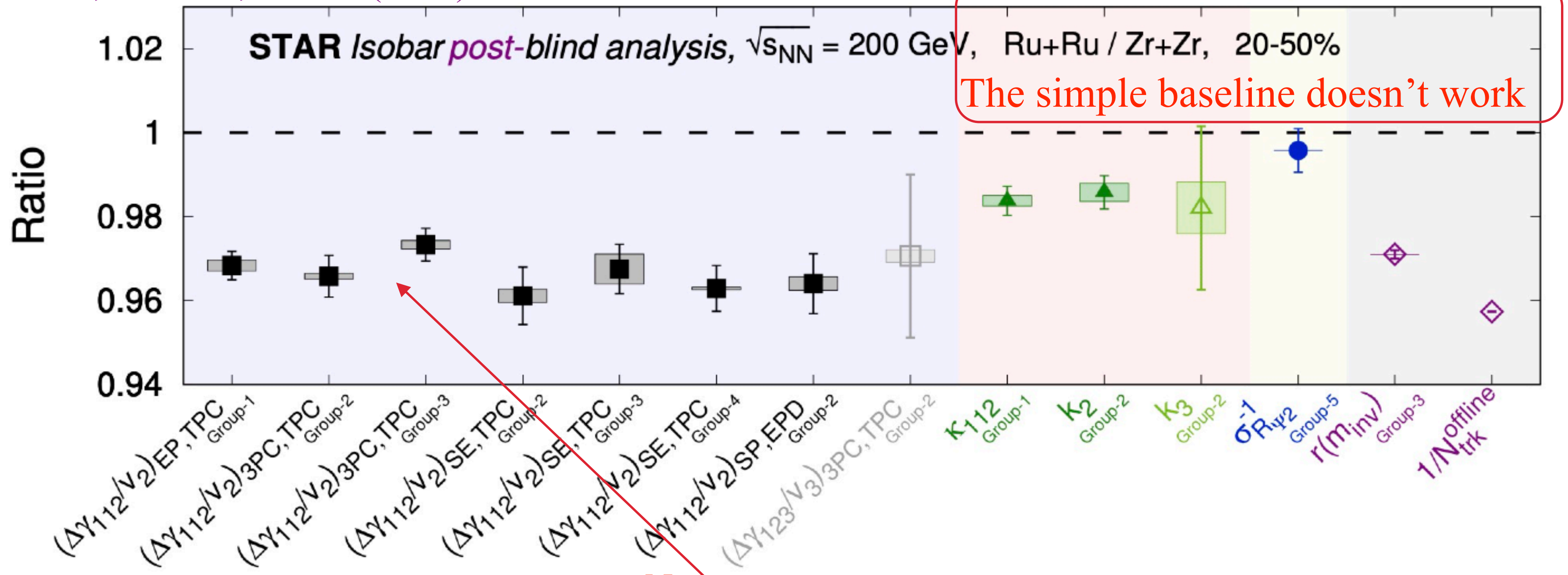

$$\Delta\gamma_{\rm bkg} = \langle \cos(\varphi_\alpha + \varphi_\beta - 2\Psi_{RP}) \rangle = \frac{N_{\rm cluster}}{N_\alpha N_\beta} \times \langle \cos(\varphi_\alpha + \varphi_\beta - 2\Psi_{\rm cluster}) \rangle \times v_{2,\rm cluster}$$

Multiplicity differences

Flow differences

The multiplicity and v2 differences from isobar structure are crucial for the CME search in the isobar collisions at RHIC

Neutron skin and symmetry energy

Charge density ≠ nuclear density.

Nuclear density distribution:

- Proton distribution — Can be accurately measured in experiment.
- Neutron distribution — Poorly known

Neutron skin: RMS radii differences between neutron distribution and proton distribution

$$\Delta r_{np} \equiv \sqrt{\langle r_n^2 \rangle} - \sqrt{\langle r_p^2 \rangle}$$

Neutron skin depends on symmetry energy:

$$E(\rho,\delta) = E_0(\rho) + E_{\rm sym}(\rho)\delta^2 + O(\delta^4)$$

$$\rho = \rho_n + \rho_p;\ \delta = \frac{\rho_n - \rho_p}{\rho}$$

$$L(\rho_c) = 3\rho_c \left[\frac{dE_{\rm sym}(\rho)}{d\rho}\right]_{\rho=\rho_c} ;\ \rho_c \simeq 0.11 {\rm fm}^{-3}$$

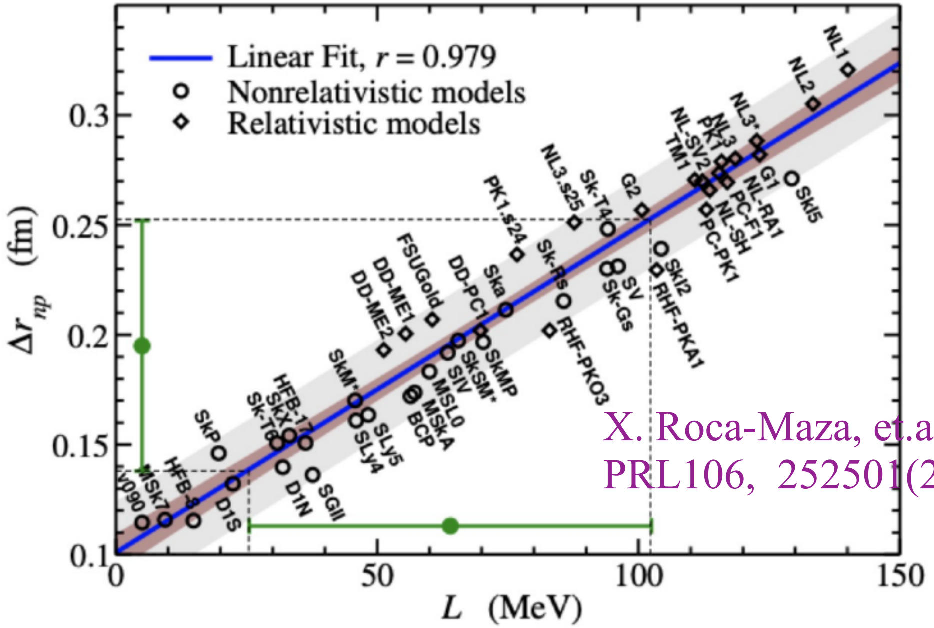

X. Roca-Maza, et.al., PRL106, 252501(2011)

The symmetry energy is crucial to our understanding of the masses and drip lines of neutron-rich nuclei and the equation of state (EOS) of nuclear and neutron star matter.

Charge densities and nuclear density in isobar collisions

- **Charge density ≠ nuclear density.**

Normally we assume neutron density profile = proton's. It's mostly ok, but for the CME search where the signal is small and we rely on large cancellation of backgrounds between two systems, we should take the difference between neutron and proton densities into consideration.

HJX, et.al., PRL121, 022301 (2018)
H. Li, HJX, et.al., PRC98, 054907(2018)

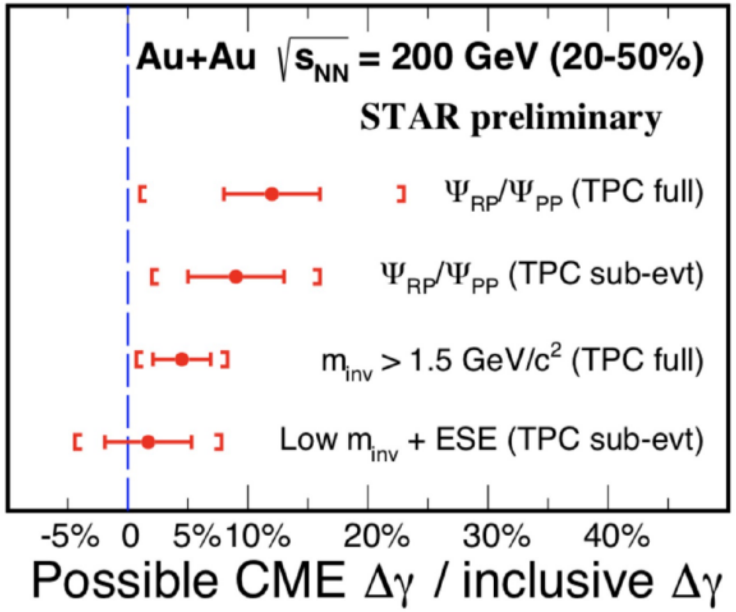

STAR Collaboration, NPA982, 535(2019)

Background dominated
--- The CME signal, if exist, is very small

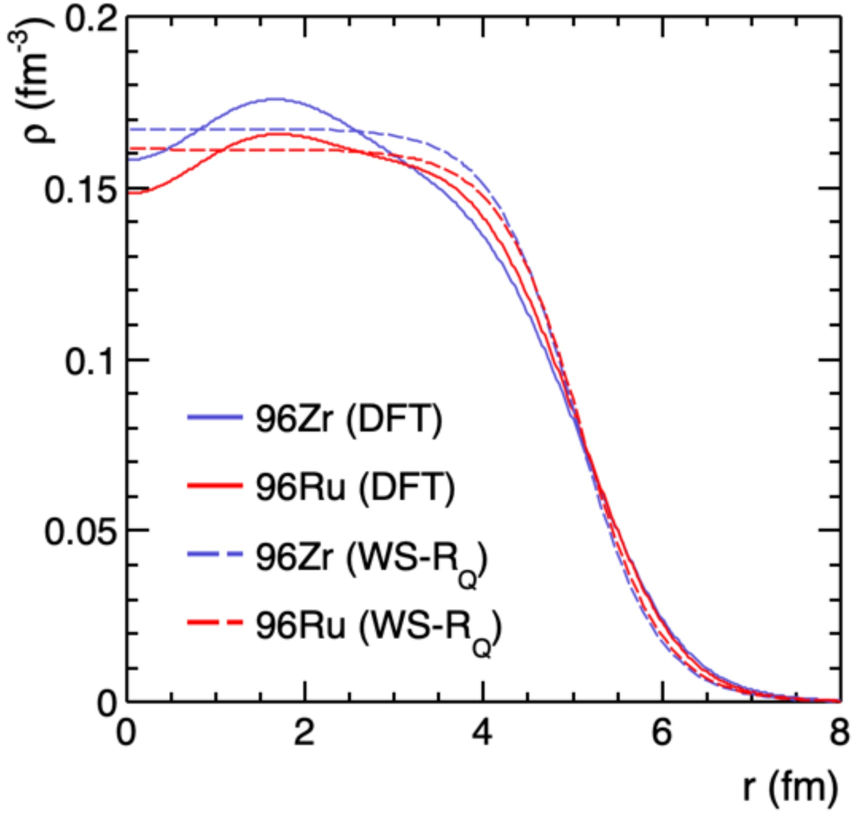

- Instead of the WS densities with parameters extracted from the measured charge densities, we use the proton and neutron densities obtained from the energy density functional theory (DFT) with Skyrme parameter set SLy4.

Multiplicity distribution difference between isobars

Predictions with charge densities

W. Deng, et.al., PRC94,041901(2016)

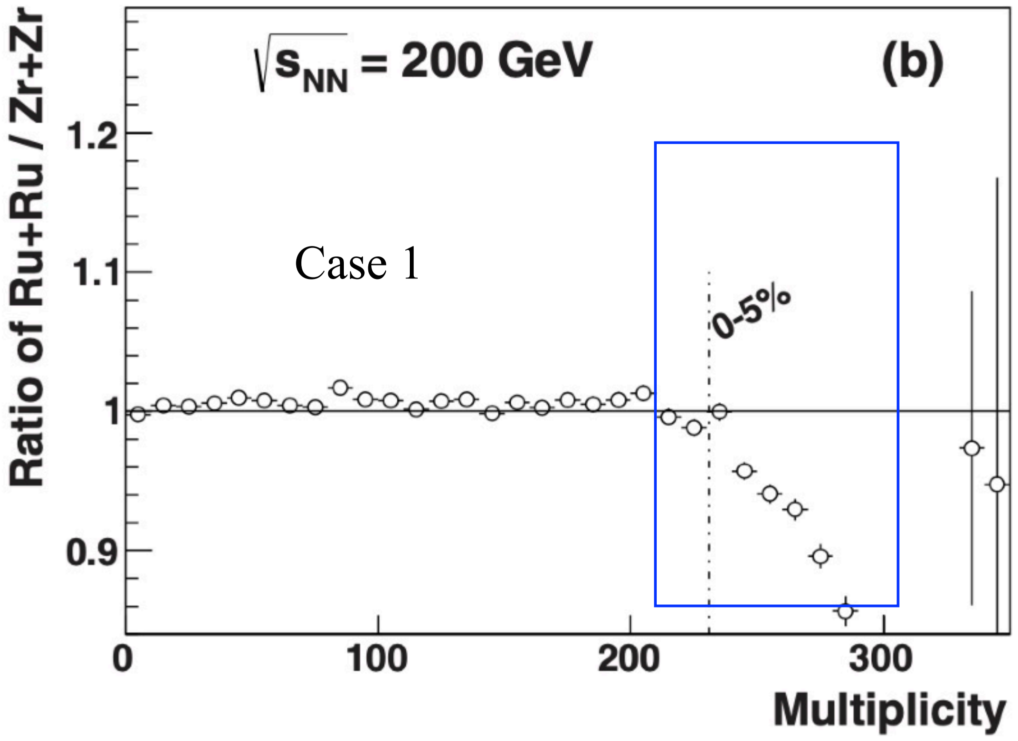

Predictions with DFT densities

H. Li, HJX, et.al., PRC98, 054907(2018)

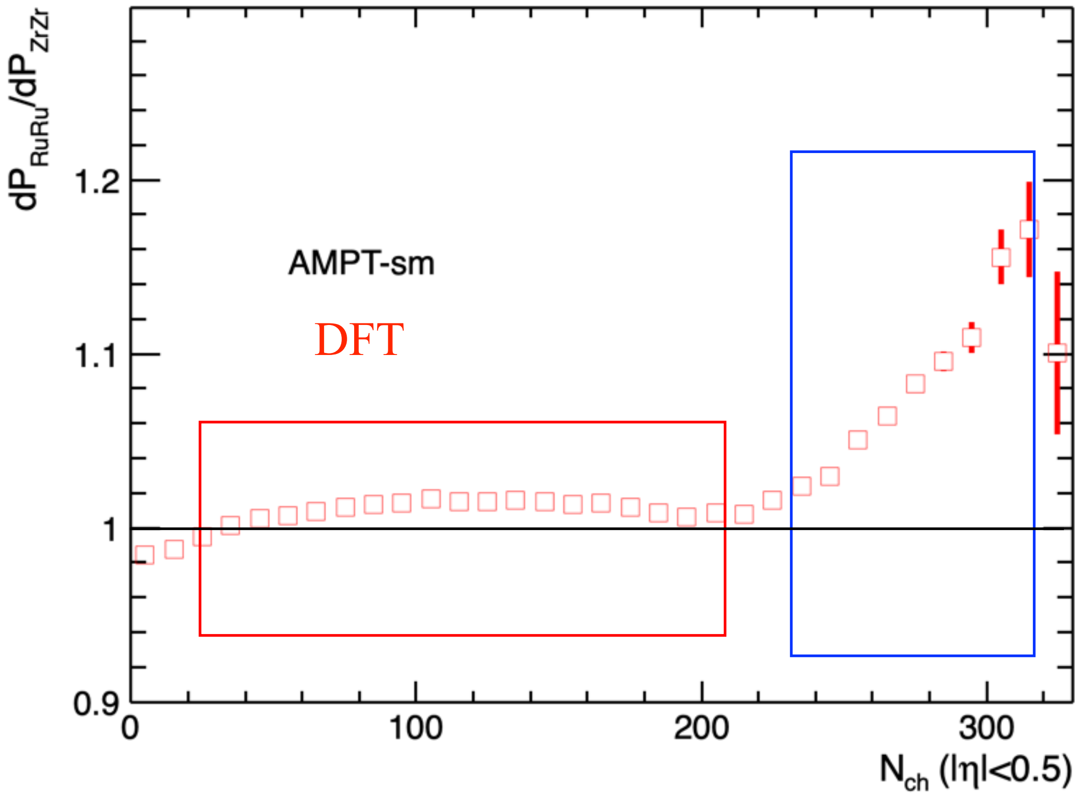

Opposite predictions from WS charge densities and DFT densities (neutron skins)

v_2 difference between isobars

Predictions from charge densities with deformation

W. Deng, et.al., PRC94,041901(2016)

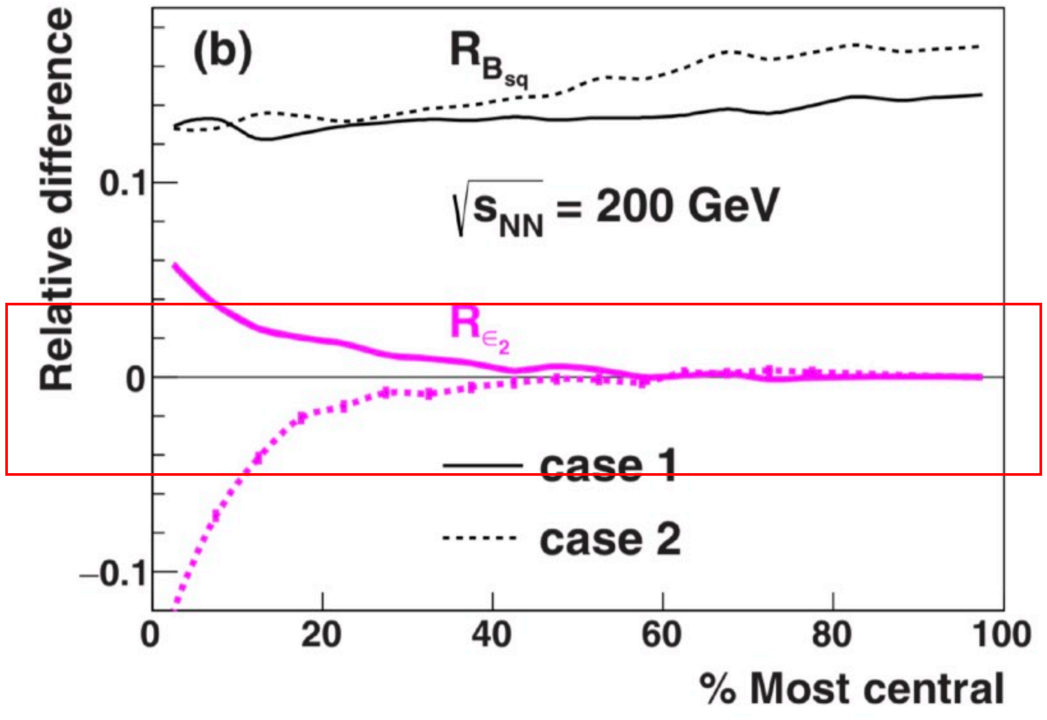

Predictions from DFT densities without deformation

HJX, et.al., PRL121, 022301 (2018)

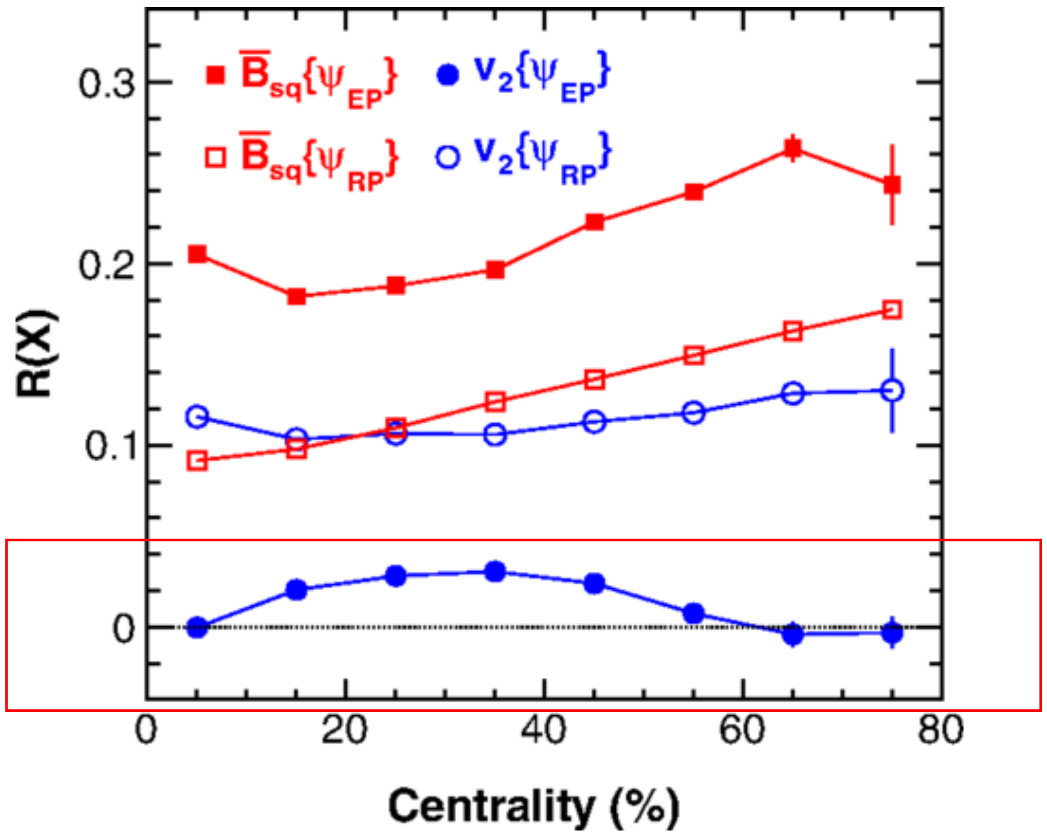

Compare to the predictions from charge densities, the calculations with DFT densities indicate that the Zr+Zr collisions and Ru+Ru collisions **have sizable differences in v_2 in 20-50% centrality range**.

Determine the neutron skin type by STAR data

HJX, et.al., PLB819, 136453 (2021)

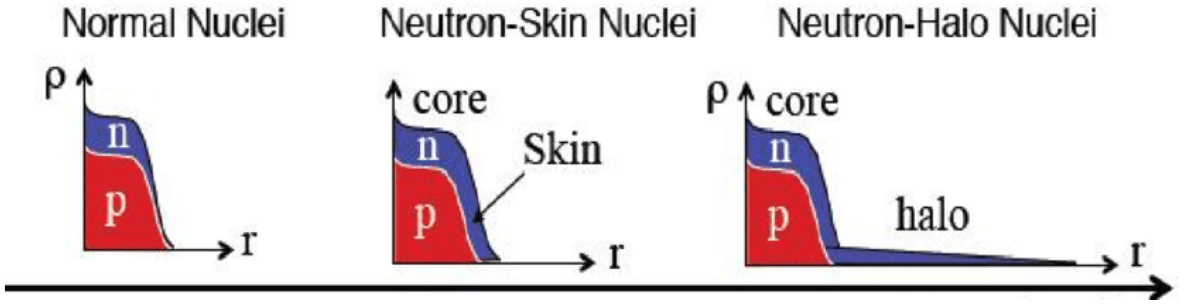

- Neutron-skin nuclei and neutron-halo nuclei for Zr

	^{96}Ru		^{96}Zr	
	R	*a*	*R*	*a*
p	5.085	0.523	5.021	0.523
skin-type n	5.085	0.523	5.194	0.523
halo-type n	5.085	0.523	5.021	0.592

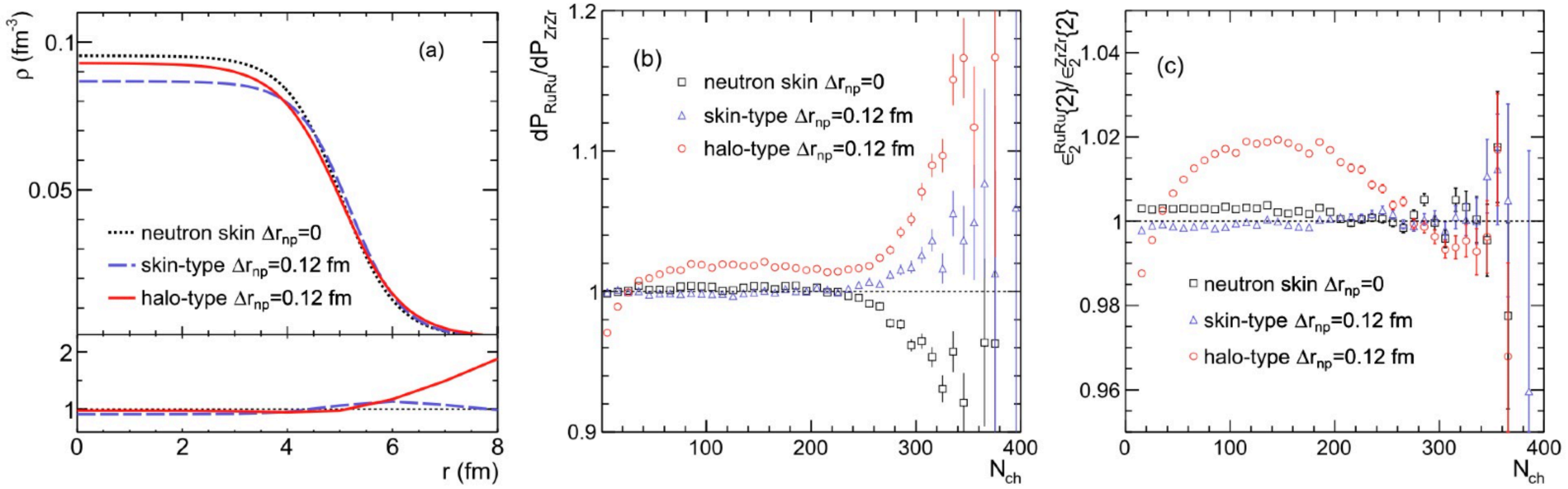

The shapes of the Ru+Ru/Zr+Zr ratios of the multiplicity and eccentricity in mid-central collisions can further distinguish between skin-type and halo-type neutron densities.

DFT predictions are verified by STAR data

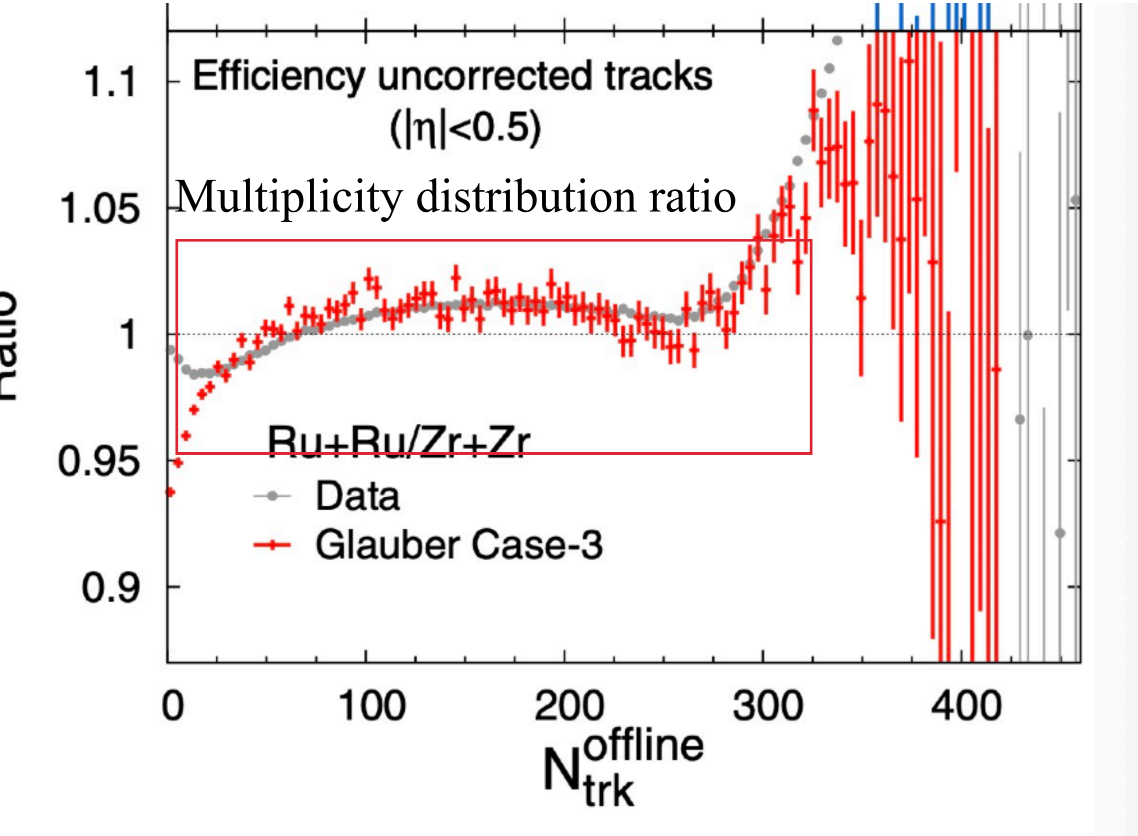

STAR, Isobar, PRC105, 014901(2022)

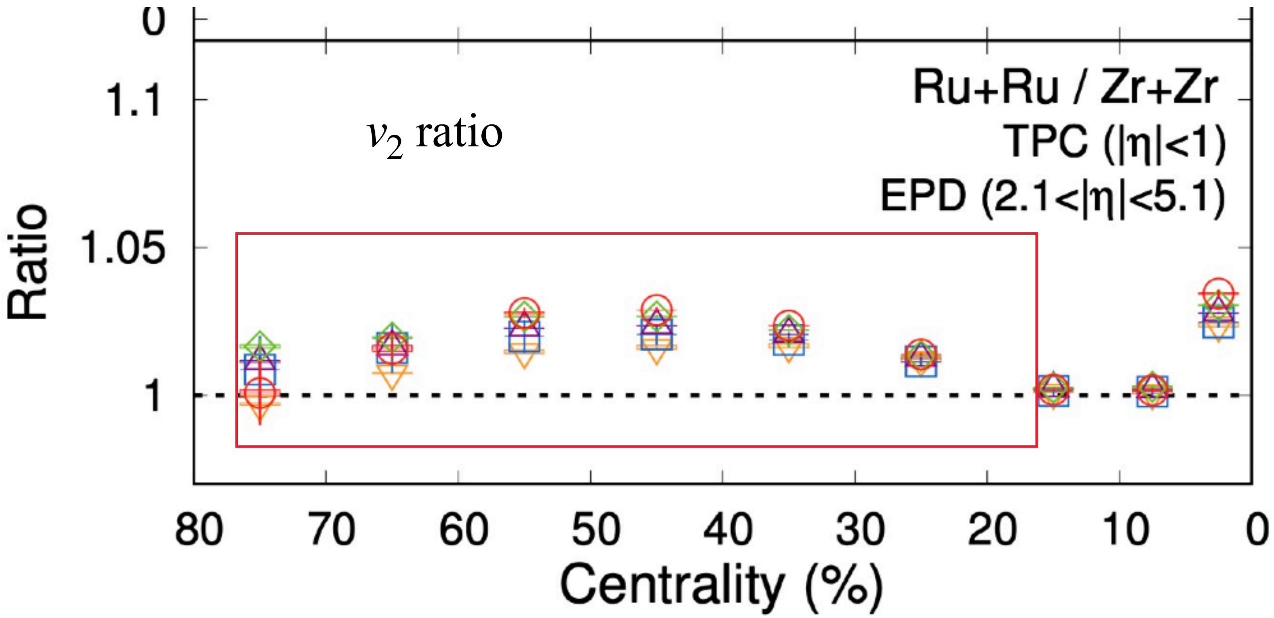

- STAR data demonstrate a thick neutron skin for the Zr nucleus, consistent with DFT predictions
- STAR data demonstrate a halo-type neutron skin, also consistent with DFT predictions

DFT predictions are verified by STAR data

H. Li, HJX, et.al., PRC98, 054907(2018)

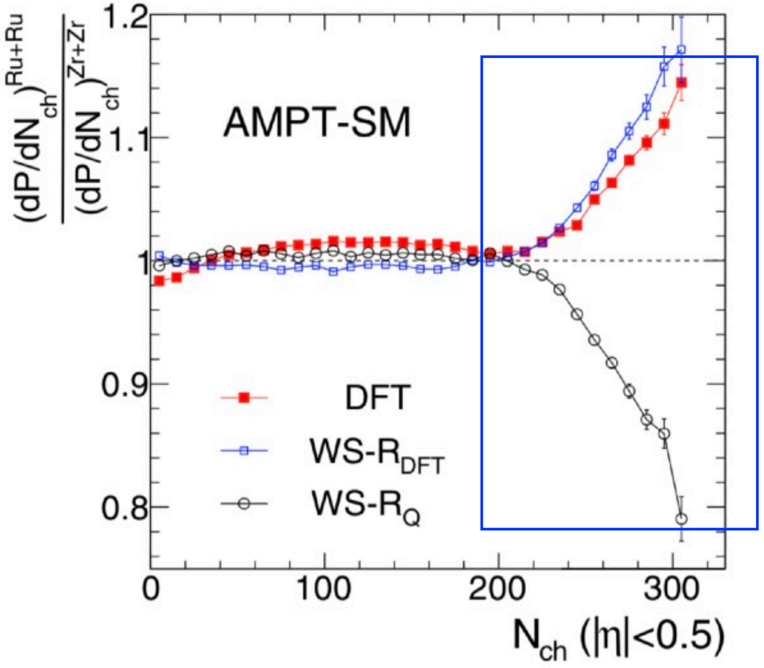

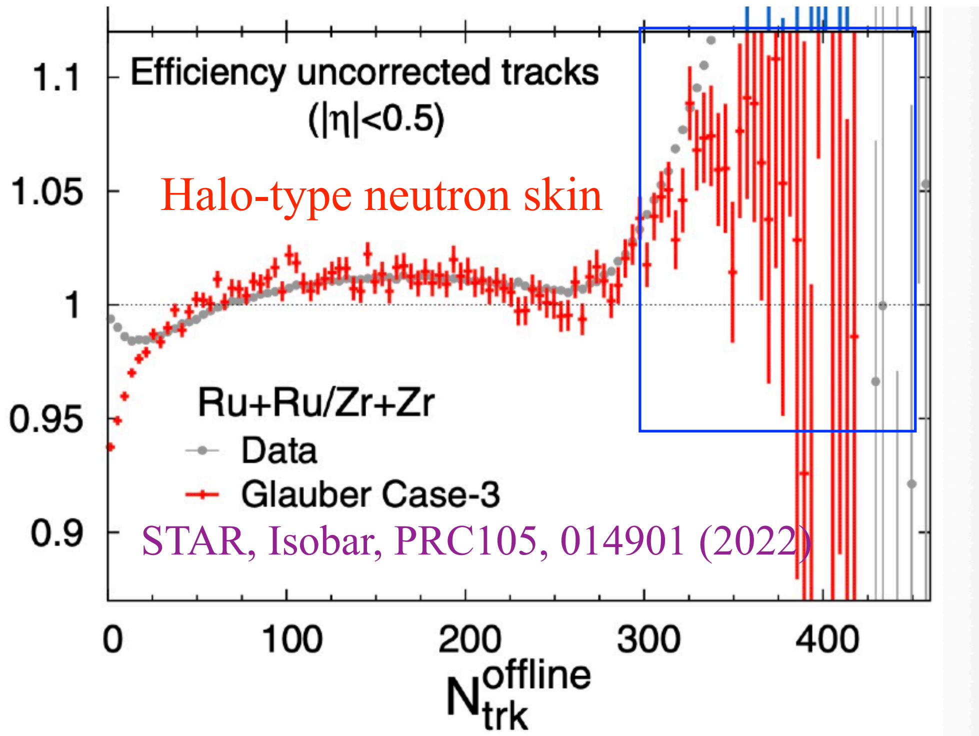

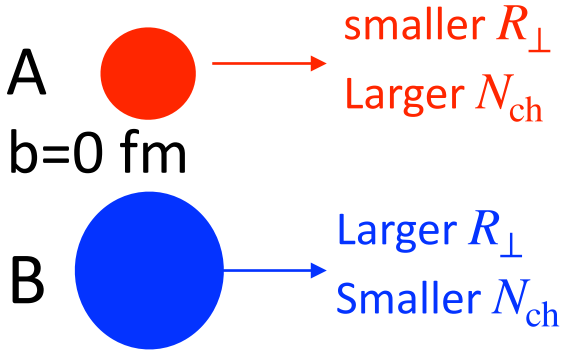

$$\left(\sqrt{\langle r_{ch}^2\rangle}\right)_{Ru} > \left(\sqrt{\langle r_{ch}^2\rangle}\right)_{Zr}$$

$$\left(\sqrt{\langle r_{DFT}^2\rangle}\right)_{Ru} < \left(\sqrt{\langle r_{DFT}^2\rangle}\right)_{Zr}$$

- The previous WS parameters extracted from charge density distributions (Ru larger than Zr) give opposite behavior to data
- The DFT densities give the correct behavior of the data ratio, because Ru is smaller than Zr from DFT calculation.
- The WS densities with the R parameter adjusted to the effective DFT radii (skin-type) give similar prediction on the tail but miss the medium multiplicity range.

Probing the neutron structure with relativistic isobaric collisions

- Neutron skin
  - Multiplicity ratio
  - $\langle p_T \rangle$ ratio
  - Net-charge ratio in very peripheral collisions
- Initial fluctuations/correlations

Current status of neutron skin measurements

PREX-2 Collaboration, PRL126, 172502(2021); B. Reed, et.al., PRL126, 172503(2021)

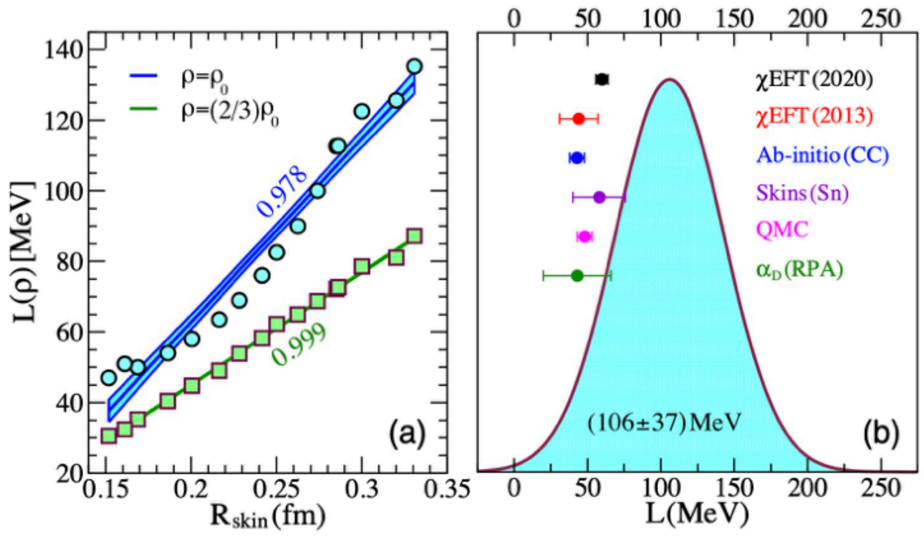

FIG. 1. Left: slope of the symmetry energy at nuclear saturation density ρ_0 (blue upper line) and at $(2/3)\rho_0$ (green lower line) as a function of R_{skin}^{208}. The numbers next to the lines denote values for the correlation coefficients. Right: Gaussian probability distribution for the slope of the symmetry energy $L = L(\rho_0)$ inferred by combining the linear correlation in the left figure with the recently reported PREX-2 limit. The six error bars are constraints on L obtained by using different theoretical approaches [14,19–25].

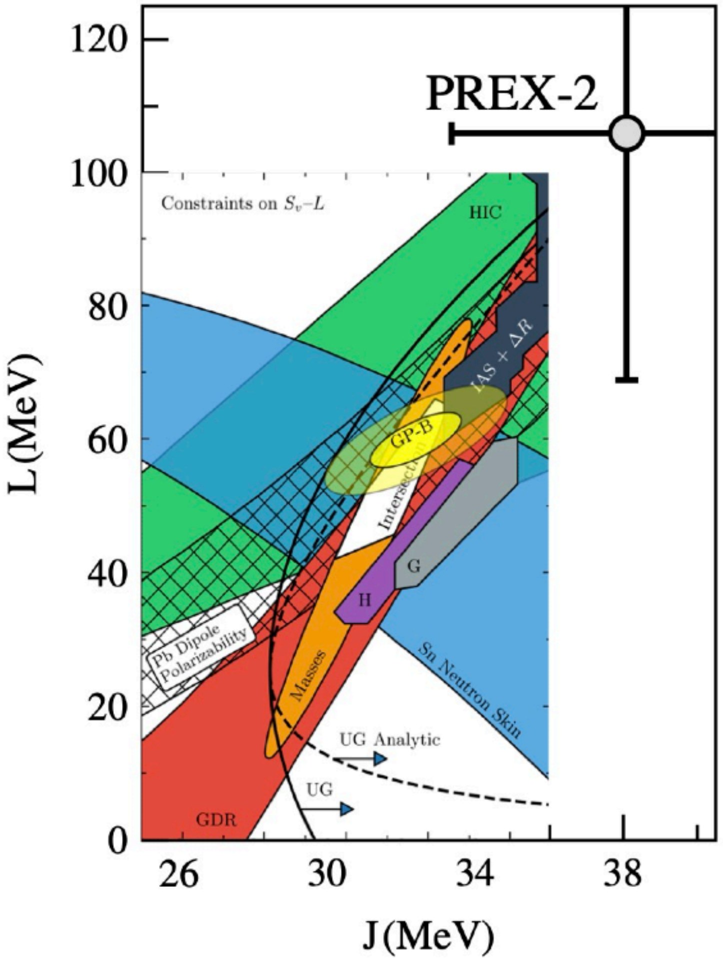

$$\Delta r_{\mathrm{np}}^{\mathrm{Pb}} = (0.284 \pm 0.071)\ \mathrm{fm}$$

$$L(\rho_0) = (106 \pm 37)\ \mathrm{MeV}$$

$$L(\rho_c) = (71.5 \pm 22.6)\ \mathrm{MeV}$$

This PREX-2 result favors a large neutron skin thickness and symmetry energy slope parameter, at tension with existing experimental data and theoretical analyses.

Neutron skin and nuclear symmetry energy

H. Li, HJX, et.al., PRL125, 222301(2020)

SHF: Standard Skyrme-Hartree-Fock (SHF) model
eSHF: Extended SHF model

$$E(\rho,\delta) = E_0(\rho) + E_{\rm sym}(\rho)\delta^2 + O(\delta^4)$$

$$\rho = \rho_n + \rho_p;\ \ \delta = \frac{\rho_n - \rho_p}{\rho}$$

$$L(\rho_c) = 3\rho_c \left[\frac{dE_{\rm sym}(\rho)}{d\rho}\right]_{\rho=\rho_c};\ \ \rho_c \simeq 0.11{\rm fm}^{-3}$$

Z. Zhang, PRC94, 064326(2016)

$$\begin{aligned} v_{i,j} &= t_0(1+x_0P_\sigma)\delta(\boldsymbol{r}) + \frac{1}{6}t_3(1+x_3P_\sigma)\rho^\alpha(\boldsymbol{R})\delta(\boldsymbol{r}) \\ &+ \frac{1}{2}t_1(1+x_1P_\sigma)[K'^2\delta(\boldsymbol{r}) + \delta(\boldsymbol{r})K^2] \\ &+ t_2(1+x_2P_\sigma)\boldsymbol{K}'\cdot\delta(\boldsymbol{r})\boldsymbol{K} \\ &+ \frac{1}{2}t_4(1+x_4P_\sigma)[K'^2\delta(\boldsymbol{r})\rho(\boldsymbol{R}) + \rho(\boldsymbol{R})\delta(\boldsymbol{r})K^2] \\ &+ t_5(1+x_5P_\sigma)\boldsymbol{K}'\cdot\rho(\boldsymbol{R})\delta(\boldsymbol{r})\boldsymbol{K} \\ &+ iW_0(\boldsymbol{\sigma}_i+\boldsymbol{\sigma}_j)\cdot[\boldsymbol{K}'\times\delta(\boldsymbol{r})\boldsymbol{K}], \end{aligned} \quad (4)$$

Extended

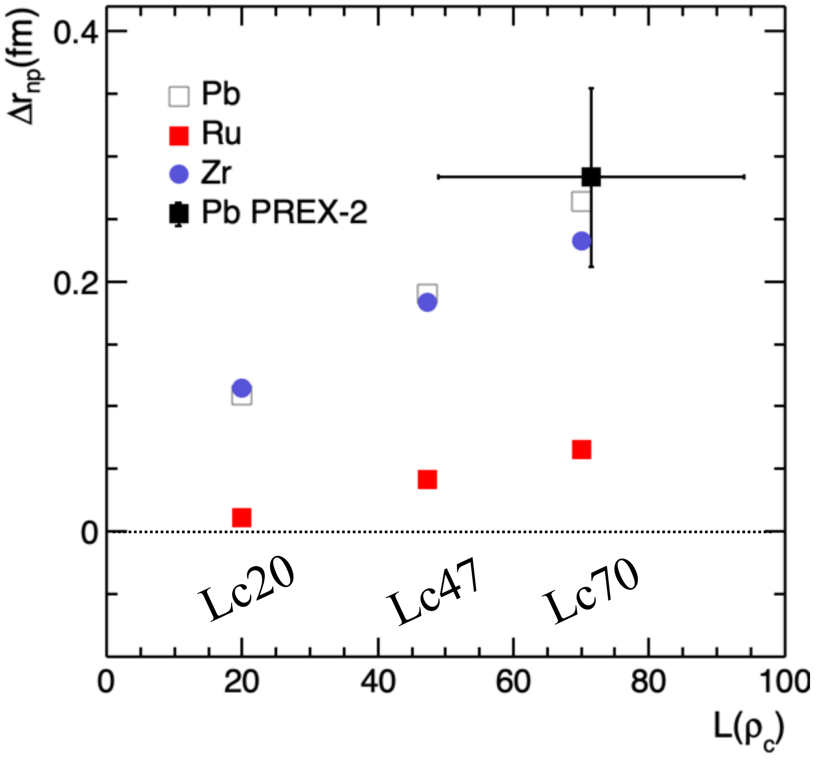

			^{96}Zr			^{96}Ru			^{208}Pb
	$L(\rho_c)$	$L(\rho_0)$	r_n	r_p	$\Delta r_{\rm np}$	r_n	r_p	$\Delta r_{\rm np}$	$\Delta r_{\rm np}$
Lc20	20	13.1	4.386	4.27	0.115	4.327	4.316	0.011	0.109
Lc47	47.3	55.7	4.449	4.267	0.183	4.360	4.319	0.042	0.190
Lc70	70	90.0	4.494	4.262	0.232	4.385	4.32	0.066	0.264
SLy4	42.7	46.0	4.432	4.271	0.161	4.356	4.327	0.030	0.160

Method I: multiplicity distribution ratio

H. Li, HJX, et.al., PRL125, 222301(2020)

Lc47: DFT calculations using data from terrestrial nuclear experiments and astrophysical observations.
Y. Zhou, L. Chen, Z. Zhang, PRD99, 121301R(2021)

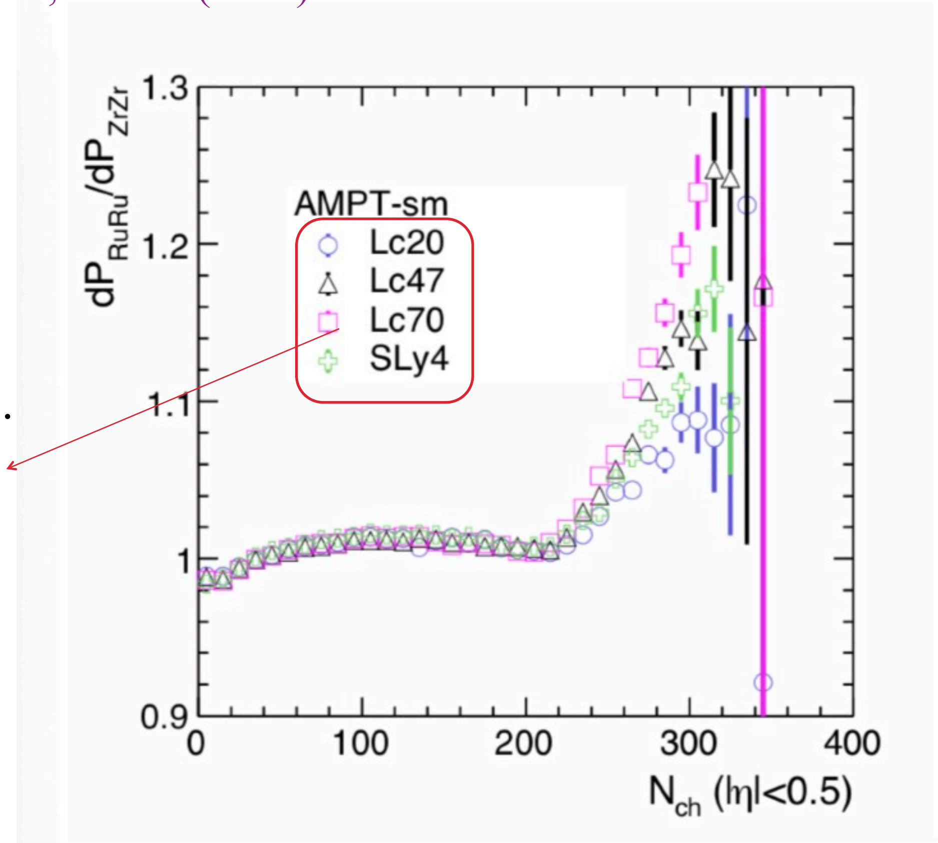

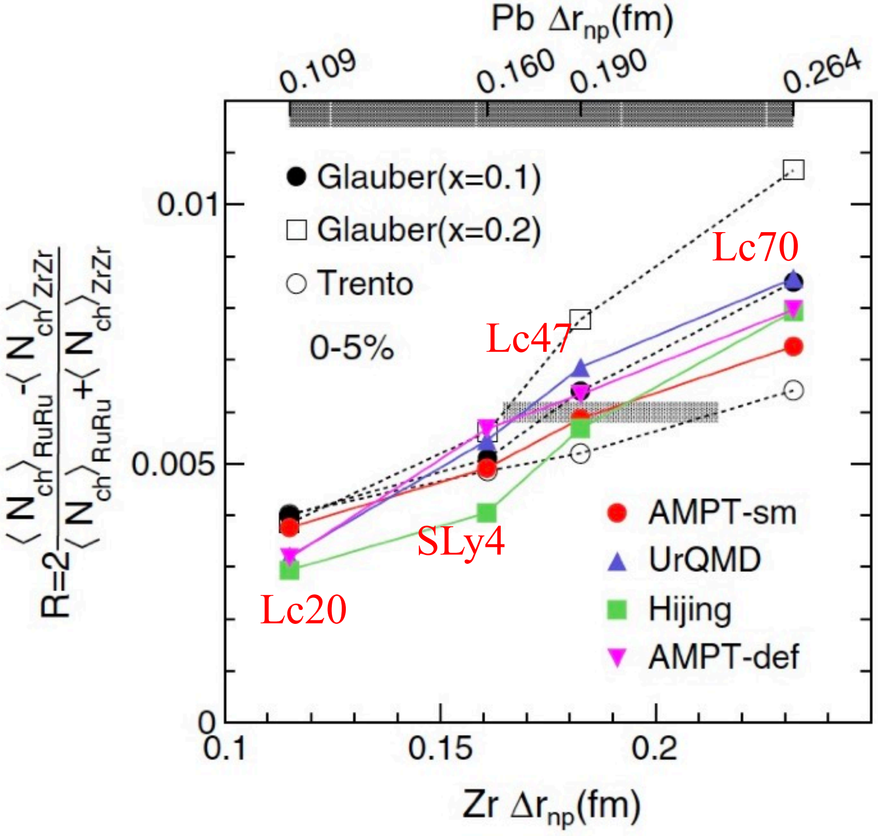

- The ratio of N_{ch} distributions highlight the differences
- To quantify the differences, we use the R observable of N_{ch} at top 5% centrality.
- R is a relative measure, **much of experimental effects cancel**
- Deformation has an effect on the tail. Quantitative investigation underway.

Method II: mean p_T ratio

HJX, et.al, arXiv:2111.14812

b=0 fm

A 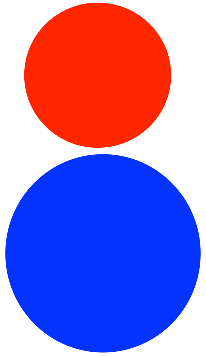 B

A → smaller $R_\perp$ → larger N_{ch} and $\langle p_T \rangle$

B → Larger $R_\perp$ → Smaller N_{ch} and $\langle p_T \rangle$)

$$R(\langle p_T \rangle) \propto R(d_\perp) \propto 1/R(\langle \sqrt{r^2} \rangle)$$

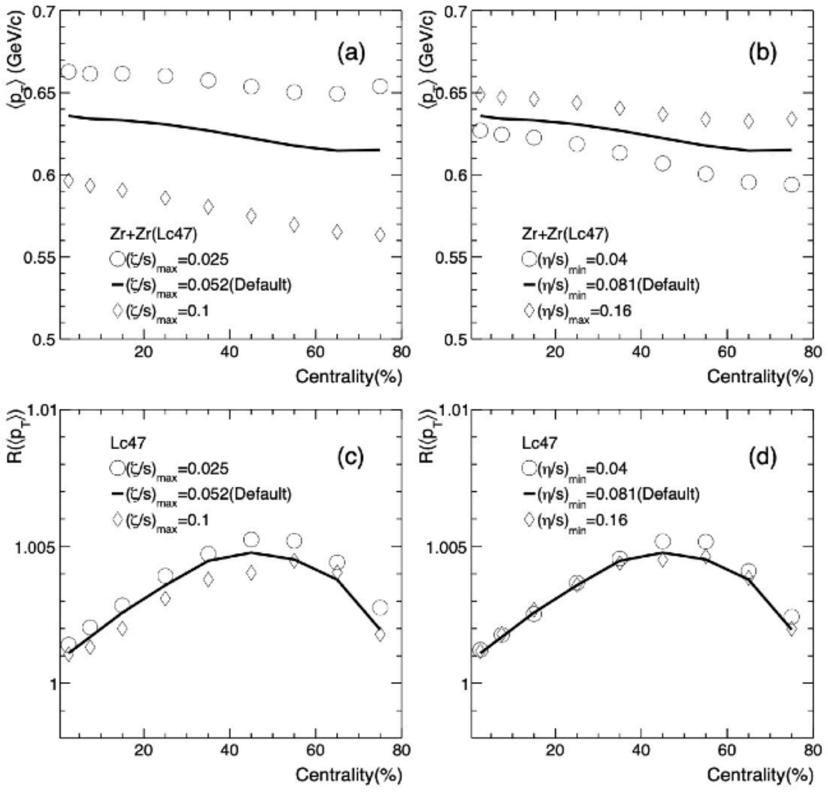

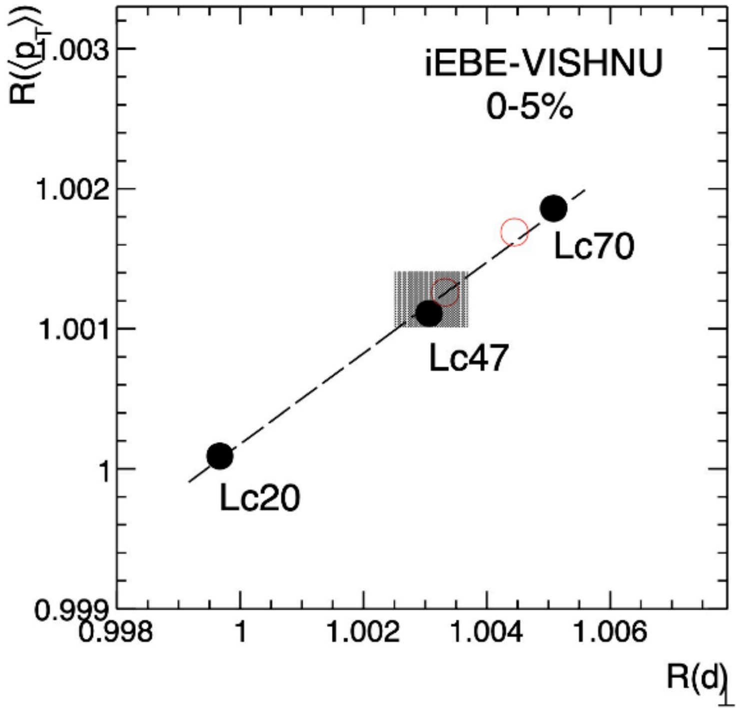

The $R(\langle p_T \rangle)$ is inversely proportional to nuclear size ratio in most central collisions.

Method III: net-charge ratio in very peripheral collisions

HJX, et.al., PRC105, L011901 (2022)

For the colliding nuclei with large neutron skin thickness

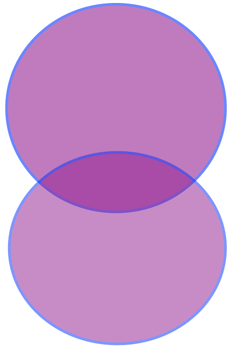

→ more n+n collisions at most peripheral collisions → Less participant charges, thus less final net-charges

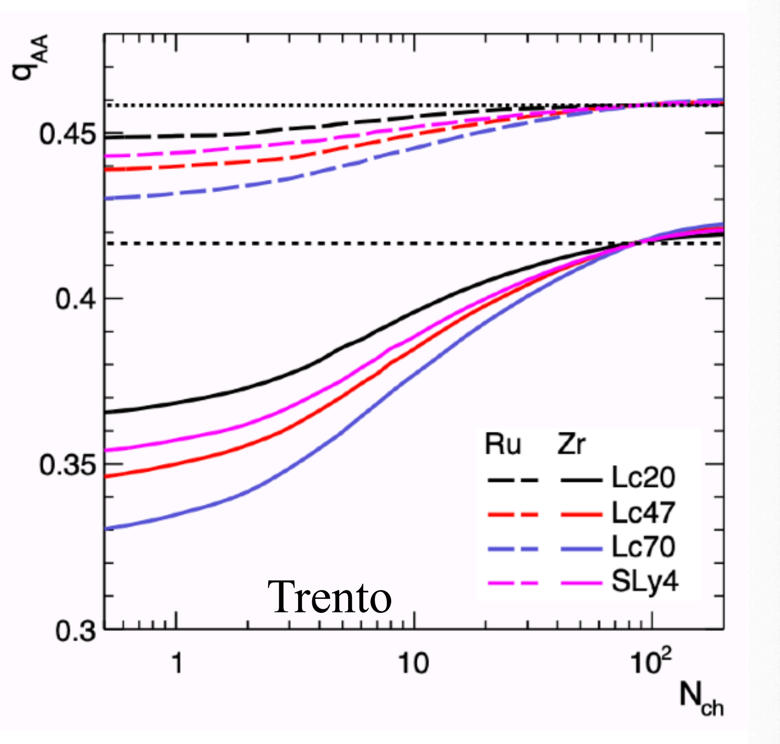

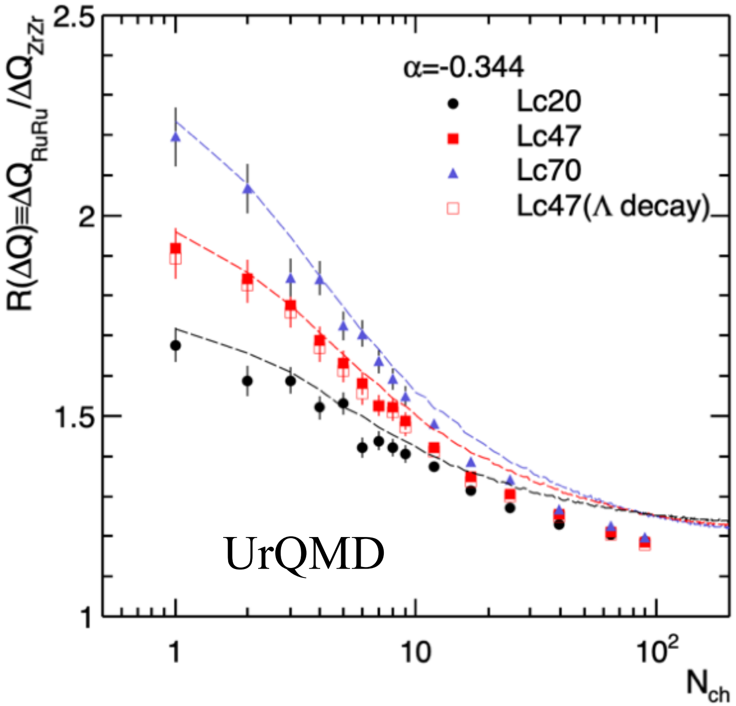

The curves are calculated by superimposition assumption

$$R(\Delta Q) = \frac{q_{RuRu} + \alpha/(1-\alpha)}{q_{ZrZr} + \alpha/(1-\alpha)}$$

where $q_{RuRu/ZrZr}$ are the fraction of protons among the participant nucleons, obtained by the Trento model.

α is the ΔQ ratio in nn to pp interaction:

Pytha: $\alpha = -0.352$

Hijing: $\alpha = -0.389$

UrQMD: $\alpha = -0.344$

Importance of initial fluctuation

STAR, Isobar, PRC105, 014901(2022)
C. Zhang, J. Jia, PRL128, 022301(2022)

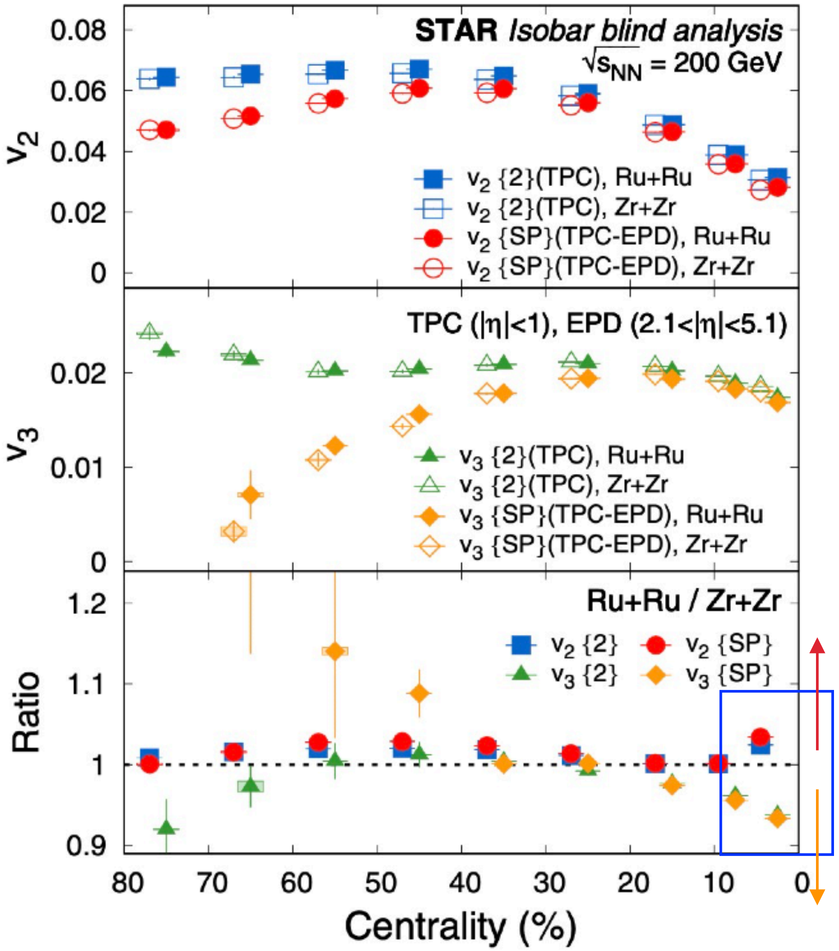

Sizable v_2 and v_3 ratios in most central collisions may indicate shape difference in isobars.

J. Wang, HJX, et.al, in preparation

^{96}Ru				^{96}Zr			
ρ_0	R	a	β_2	ρ_0	R	a	β_3
0.159	5.093	0.488	0.00	0.163	5.022	0.538	0.00
0.159	5.090	0.473	0.16	0.163	5.016	0.527	0.16

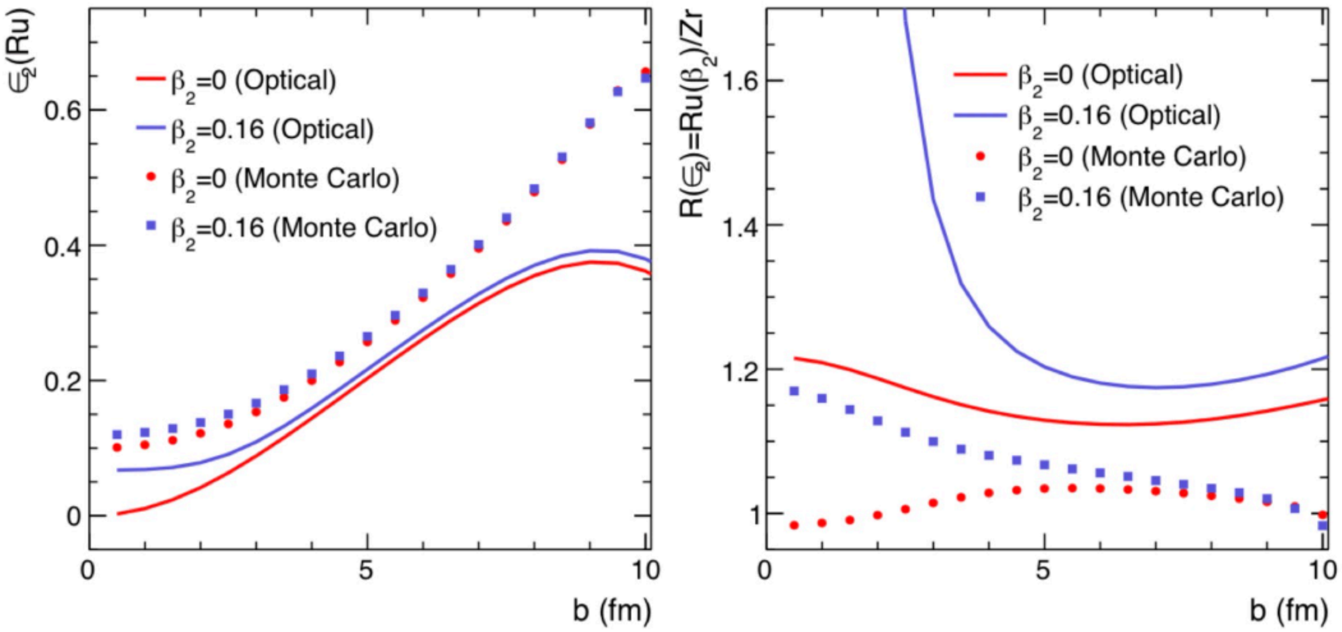

The initial fluctuation significant dilute the geometry differences from nuclear densities
Fluctuation modeling is important.

Importance of initial fluctuation

G. Giacalone, et.al, arXiv:2111.02908

J. Wang, HJX, et.al, in preparation

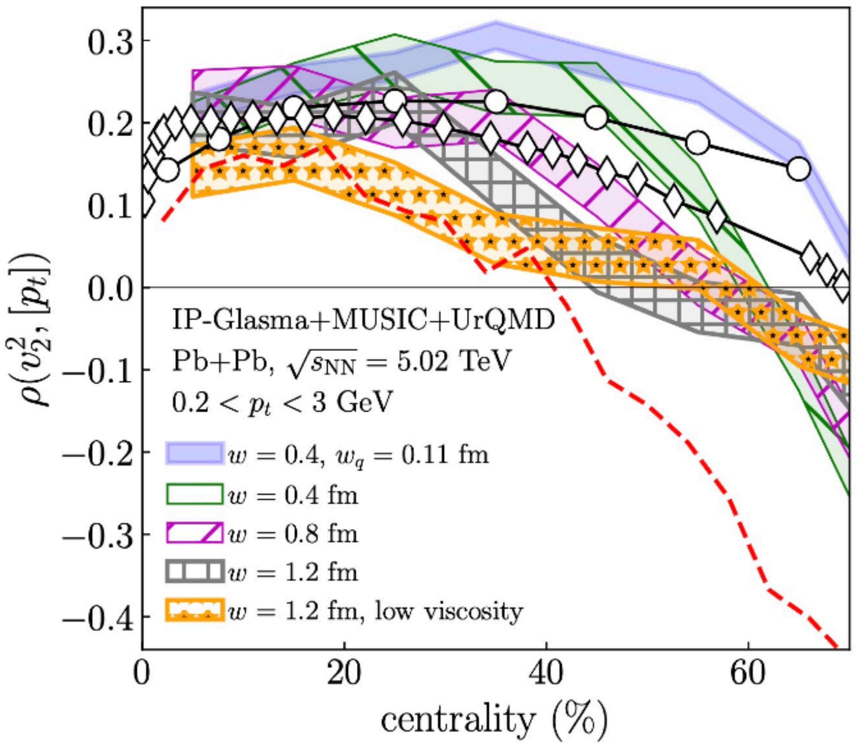

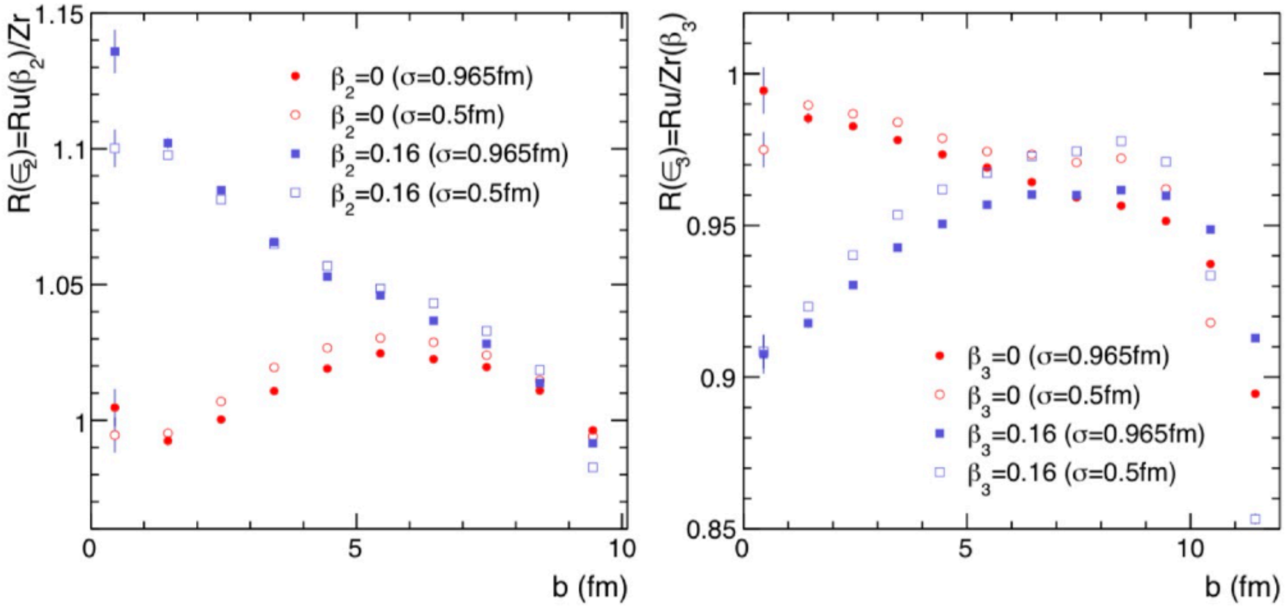

The nucleon width parameter has sizable contributions to the third order eccentricity (anisotropic flow) differences.

$$\rho_n \equiv \rho(v_n^2, [p_t]) = \frac{\langle \delta v_n^2 \delta [p_t] \rangle}{\sqrt{\langle (\delta v_n^2)^2 \rangle \langle (\delta [p_t])^2 \rangle}},$$

Effect of hydrodynamic response

G. Nijs, W. van der Schee, arXiv:2112.13771

J. Wang, HJX, et.al, in preparation

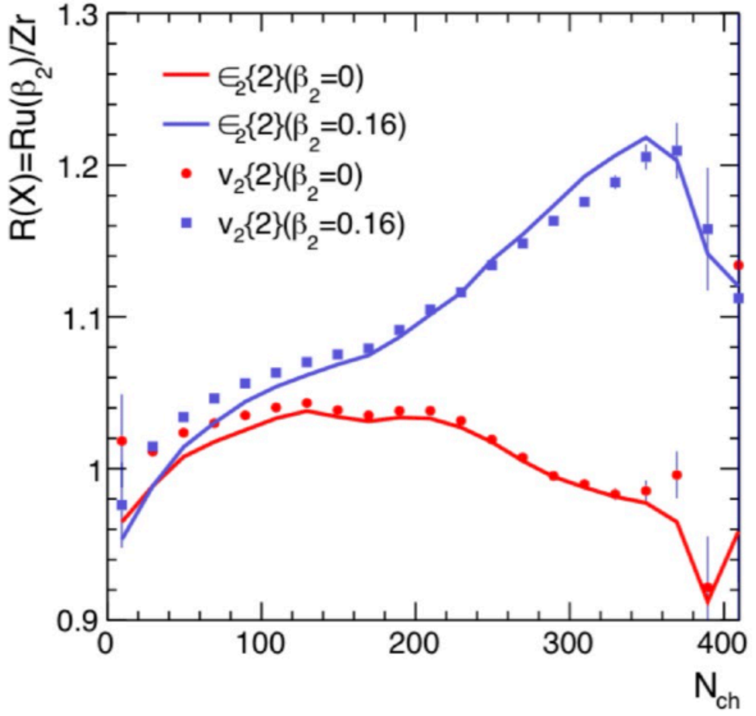

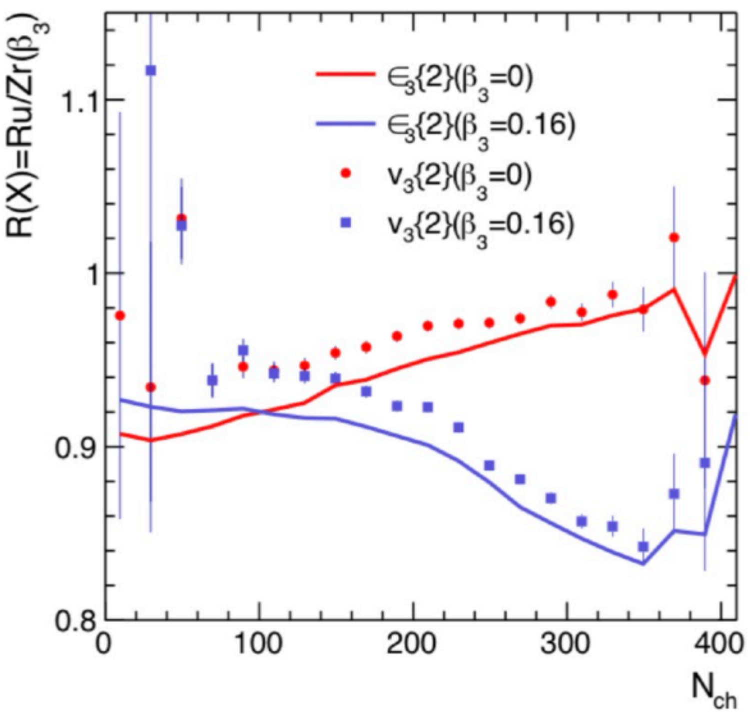

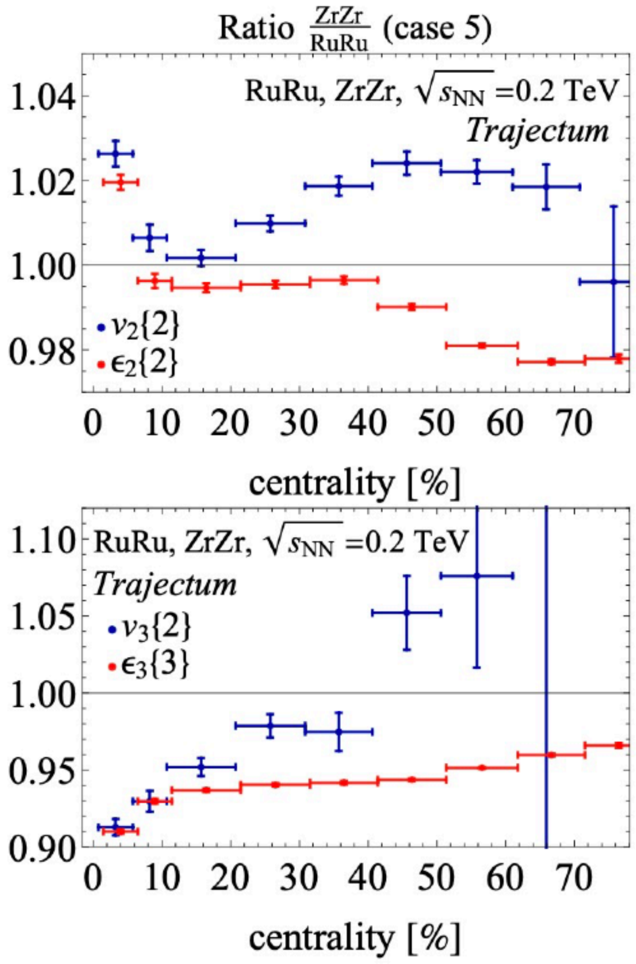

The hydrodynamic evolution can further bias the eccentricity differences, especially for the third order eccentricity (anisotropic flow)

Need further investigations in order to understand the flow difference in isobar systems

SUMMARY

- The STAR isobar data demonstrate **thick halo-type neutron skin in Zr**, consistent with **DFT** calculations
  - Nuclear structure causes isobar multiplicity and v2 differences, important for the CME search
- Relativistic isobar collisions can be used to **probe the neutron skin and symmetry energy**
  - Multiplicity distribution ratio; Mean p_T ratio; Net charge ratio

Deformation requires investigation of fluctuation effects on flow difference

Thank you for your attention!

Haojie Xu(徐浩洁)

Huzhou University(湖州师范学院)

Backup

Deformation effect